



## Review

## Identifying of charge-transfer transitions and reactive centers in M(diimine)(dithiolate) complexes by DFT techniques

Christiana A. Mitsopoulou\*

*Inorganic Chemistry Laboratory, Chemistry Department, National and Kapodistrian University of Athens, Panepistimiopolis, Zografou 157 71, Greece*

## Contents

1. Introduction .....	1449
2. Square-planar mixed-ligand diimine–dithiolate complexes .....	1449
2.1. Molecular structure .....	1449
2.2. Electronic transitions and excited states of M(diimine)(dithiolate) complexes: effect of metal, ligands and solvent .....	1451
2.2.1. Ground and singlet states .....	1451
2.2.2. Triplet states and emission spectra .....	1453
3. Calculated indices at DFT level for M(diimine)(dithiolate) complexes .....	1453
3.1. The NICS index: measuring the extent of the delocalization in the molecular plane .....	1453
3.2. Fukui functions: searching the reactive centers in a molecule .....	1454
4. Conclusions .....	1455
Acknowledgements .....	1455
References .....	1455

## ARTICLE INFO

## Article history:

Received 27 August 2009

Accepted 22 December 2009

Available online 13 January 2010

## Keywords:

Dithiolato and dithiolene ligands

Diimine ligands

DFT technique

Excited states

Fukui

NICS

Stacking interactions

## ABSTRACT

This review is focused on theoretical aspects of mixed diimine–dithiolate complexes by means of DFT and TD-DFT methods. Thus, the geometry, the character of charge-transfer transitions and excited states in a series of M(diimine)(dithiolate), where M = Ni, Pd and Pt, is examined by DFT and TD-DFT techniques combined with polarized continuum model. The theoretical calculations reveal not only the role of the ligands – namely diimine and dithiolato and their substituents – but also the role of the metal in the excited triplet and singlet states and as a consequence in the properties of these complexes (electronic and photophysics) and their potential use as photosensitizers, NLO materials, light energy conversion materials and biological agents. The calculated energies of the lowest triplet and singlet state in all these complexes are in good agreement with absorption spectra and luminescence studies—where they are available. The contribution of the metal in the chemical and photophysics properties of this class of compounds is also demonstrated by two indices derived by DFT techniques: NICS (for chemical) and Fukui functions (for chemical and photophysical properties). The former acts as a meter of the delocalization of these molecules whereas the latter identifies the reactive centres of the molecule. All the theoretical results are in accordance with the experimental ones—geometrical structures, absorption, luminescence and  $^1\text{H}$  NMR spectra as well as products of given reactions, indicating the applicability of the DFT and TD-DFT techniques in examining the properties of metal coordinated complexes especially in a series of the same class of compounds.

© 2010 Elsevier B.V. All rights reserved.

**Abbreviations:** bdt, 1,2-benzenedithiolate; bpy, 2,2-bipyridine; CPCM, conductor like polarizable continuum model; CT, charge transfer; dcbpy, dicarboxyl-bpy; DFT, density functional theory; edt, ethylene-1,2-dithiolate; HSAB, hard–soft acid–base principle; HOMO, highest occupied molecular orbital; ILCT, intraligand charge transfer; LLCT, ligand to ligand charge transfer; MLCT, metal to ligand charge transfer; MLLCT, metal–ligand-to–ligand charge transfer; MMLL/CT, mixed metal–ligand-to–ligand charge-transfer; mnt, maleonitriledithiolate; LUMO, lowest unoccupied molecular orbital; NICS, the nucleus independent chemical shifts; NLO, non-linear optics; pq, 2-(2'-pyridyl)quinoxaline; phen, 1,10-phenanthroline; TD-DFT, time-dependent DFT; tdt, 3,4-toluenedithiolate.

\* Tel.: +30 210 7274452; fax: +30 210 7274782.

E-mail address: [cmitsop@chem.uoa.gr](mailto:cmitsop@chem.uoa.gr).

## 1. Introduction

Over the past four decades a tremendous upsurge of interest in the chemistry of dithiolenes complexes has been observed due to their potential applications as Q-switch laser dyes [1], light energy conversion materials [2–11], non-linear optics [12,13] and as models for molybdenum pterin cofactors [14]. This wide range of applications derives from the unique electronic structures of this class of complexes [15–18] and their reversible redox behavior [19–21] and are well reviewed in the special volume 'Dithiolene Chemistry' edited by Stiefel [22].

In the recent years, among all the dithiolene complexes researchers' interest has been attracted by the M(diimine)(dithiolate) complexes of group VIII metals because of their unique properties, which include solution luminescence, solvatochromism, large molecular hyperpolarizabilities, and large excited-state oxidation potentials [23–31]. Moreover, these complexes represent a very promising class of compounds for non-linear optical (NLO) materials, in view of their peculiar electronic structure. The latter is dominated by the existence in the same molecule of the two different unsaturated chelating ligands one of which is more easily reduced (dithiolate) and the other more easily oxidized (diimine). These complexes generally absorb light in the visible and ultraviolet regions and it is possible to introduce selectively properly designed  $\alpha$ -diimine ligands and suitable co-ligands in a co-planar arrangement tailoring the molecules for potential application as photosensitizers, photocatalysts [32–34] or even biological agents [35,36]. The intense solvatochromic band in the low energy region of their electronic spectra is considered to involve the highest occupied molecular orbital (HOMO), which is a mixture of metal and dithiolate orbital character, and the lowest unoccupied molecular orbital (LUMO), which is a  $\pi^*$  orbital of the diimine and has been termed a "mixed metal-ligand-to-ligand charge-transfer" (MMLT/CT) [37,38] or MLCT/LLCT as recently has abbreviated [39–42].

Moreover, the pioneer experimental work of Eisenberg has demonstrated that the charge-transfer excited state of Pt(II) mixed diimine–dithiolate complexes is emissive, in contradiction to Pd(II), in fluid solution and undergoes electron-transfer quenching both oxidatively and reductively [25,27,28] and is attributed as  $^3$ MMLT/CT. On the other hand, Srivastava and co-workers suggested that both complexes Pt(bpy)(tdt) and Pd(bpy)(tdt) act as photosensitizers for the formation of singlet oxygen, attributing this ability to a unique LL/CT-based excited state [43]. The latter is of great importance since it has been referred that the mixed ligand complexes of Pd(II) and Pt(II) undergo photoinduced oxida-

tion in the presence of atmospheric oxygen to yield monosulfenate, disulfenate, mixed sulfinate/sulfenate, monosulfinate and disulfinate complexes [30,44–46].

The distinction between the LL/CT and MMLT/CT transition although it is specified to the percentage of metal nd orbitals to HOMO, is of great importance since the knowledge of the nature of the frontier orbitals as well as the nature of the energy transitions would be unambiguously a helpful tool in synthesis or design of functional molecules and for a mechanistic analysis of their photochemistry and electrochemistry. Thus, an appropriate choice of diimine chelate ligand, co-ligand (dithiolene or dithiolate) and metal – if it plays a role – should allow predetermination of the character of the lowest energy transitions and lowest emitting states in this class of complexes.

The assignment of the excited state of the square-planar mixed-ligand dithiolate–diimine complexes based mainly on experimental work has recently been reviewed by Cumming and Eisenberg in the book 'Dithiolene Chemistry' [22] but theoretical studies on these complexes have not yet been reviewed. On the other hand, one main target of the researchers is to tune the M(diimine)(dithiolate) properties in a formal way that could allow the prediction of properties of new compounds—even ones which have not been synthesized. For the latter to be achieved a good electronic description is of a central importance and this can be achieved by Density Functional Theory (DFT). DFT has been proven to be extremely useful to obtain almost accurate molecular orbital energies and other properties of transition metals complexes [47,48] especially if there is a comparison among the calculated properties of the compounds of the same class and the existed experimental ones [38,48]. Moreover, some theoretical calculated indices like the nucleus independent chemical shifts (NICS) [49], and Fukui functions [50] can be used to get insight into the reactivity of M(diimine)(dithiolate) complexes which certainly reflects on their electronic structure.

## 2. Square-planar mixed-ligand diimine–dithiolate complexes

### 2.1. Molecular structure

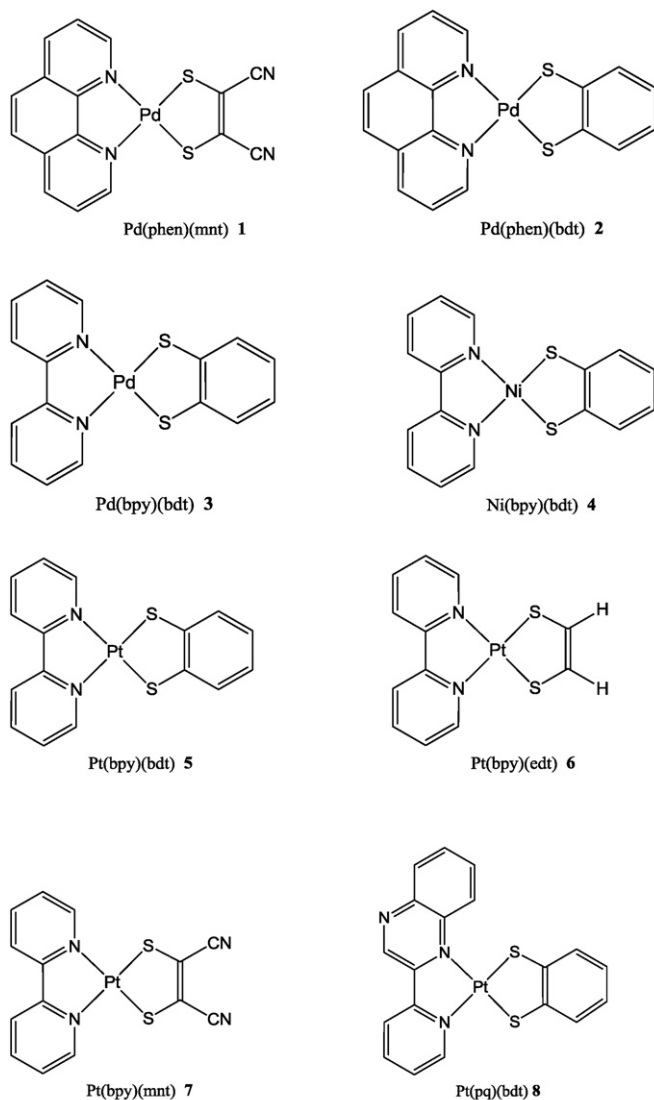
As it is not always easy to crystallize this class of complexes (up to now only fourteen crystal structures of M(diimine)(dithiolate) complexes have been reported [51]) their geometries is necessary to be optimized using DFT calculations. This could help one to reveal the role of the metal and the ligands both to the molecular and electronic structure. Selected data fully optimized using

**Table 1**

Comparison of selected calculated bond lengths (Å) and angles (deg.) for **1–8** with experimental values from X-ray analysis.

C	M	M–N <sup>a</sup>	M–S <sup>a</sup>	C–S <sup>a</sup>	C=N <sup>a</sup>	C=C <sup>dithiol.</sup>	C=C <sup>diim.</sup>	$\varphi_{\text{diim.}}$	$\varphi_{\text{dithiol.}}$
<b>1</b>	Calc.	2.128	2.282	1.762	1.363	1.363	1.434	78.87	88.62
<b>2</b>	Exp. [38]	2.096(8)	2.261(3)	1.787(10)	1.368(12)	1.376(13)	1.437(13)	80.2(3)	89.17(10)
	Calc. <sup>b</sup>	2.128	2.283	1.775	1.364	1.401	1.434	78.69	88.49
	Calc. <sup>c</sup>	2.115	2.274	1.774	1.364	1.401	1.482	79.01	88.87
<b>3</b>	Exp. [44]	2.071(2)	2.245(1)	1.762(2)	1.353(3)	1.396(3)	1.474(3)	79.41(6)	88.67(2)
	Calc. <sup>b</sup>	2.120	2.286	1.774	1.358	1.401	1.476	77.85	88.16
	Calc. <sup>c</sup>	2.103	2.263	1.769	1.354	1.399	1.475	78.15	88.43
<b>4</b>	Exp. [45]	1.937(2)	2.144(3)	1.755(3)	1.358(3)	1.395(3)	1.472(3)	83.31(8)	90.18(3)
	Calc.	1.970	2.178	1.765	1.358	1.401	1.467	82.26	90.18
<b>5</b>	Exp. [46]	2.050(5)	2.248(2)	1.761(6)	1.367(8)	1.373(8)	1.464(8)	80.1(2)	89.0(1)
	Calc. <sup>b</sup>	2.095	2.299	1.771	1.363	1.402	1.466	78.00	88.26
	Calc. <sup>c</sup>	2.085	2.269	1.760	1.363	1.387	1.466	79.02	88.47
<b>6</b>	Exp. [39]	2.049(4)	2.250(1)	1.743(7)	1.362(7)	1.346(14)	1.469(10)	79.26(16)	88.67(6)
	Calc.	2.092	2.302	1.754	1.365	1.341	1.462	78.10	88.05
<b>7</b>	Calc.	2.099	2.296	1.759	1.362	1.365	1.469	78.04	88.44
<b>8</b>	Calc. [35]	2.303	2.211	1.765	1.355	1.401	1.458	77.6	67.4

<sup>a</sup>The average value of both distances. <sup>b</sup>Without and <sup>c</sup>with polarization function for Pd and Pt, respectively.



the B3LYP/SDD/6-311+G\* level of theory are shown in Table 1 for selected complexes of the type M(diimine)(dithiolate) **1–8** (Scheme 1) and are compared with experimental ones. B3LYP was chosen as it is one of the most widely used functional mod-

els for transition metal complexes [48,52]. The basis set used for all non metal atoms was the well-known valence triple- $\zeta$  6-311+G\*[53]. The quasi-relativistic Stuttgart–Dresden effective core potential of the type ECP10MDF, ECP28MWB, ECP60MWB was used for Ni, Pd and Pt, respectively [54,55]. The core potentials were complemented by the relative valence basis sets [55]. For all other calculations related to the properties investigation, an additional diffuse and polarization function was added to the hydrogen atoms. Moreover, calculations were performed with the fully relativistic ECP28MDF [56]. The structural results of the cc-pVTZ-PP VTZ-PP basis for Pd and Pt are in good agreement with the experimental ones (Table 1) [57]. In agreement with results reported by other groups, we found that changing the basis set or the density functional had little effect on the calculated transitions and orbital compositions (Section 2.2) and certainly does not alter the order in a series of the same class of complexes [58–60]. We have also checked our results by systematical change of the computing method (HF, MP2, DFT with both hybrid and non hybrid functionals) and the employed basis sets (of double and triple zeta quality). All calculations, apart from the combination HF/6-31G\*, end qualitatively to the same results, whilst pure functionals strongly underestimate energies of CT transitions.[48]

As shown in Table 1 the optimized calculated structures of complexes **1–8** are in excellent agreement with the experimental observations. The slight overestimation of the M–X bond distances is typical for present day DFT functionals [61]. Actually, in the case that a polarization basis is used for Pd and Pt this difference is even smaller.

Variation in molecular design of the complexes **1–8**, through changes in the metal ion, diimine and dithiolate ligands, can be used to affect changes in their molecular and electronic structures. Complexes **1–7** are a square-planar, of almost  $C_{2v}$  molecular symmetry, with two five member rings (namely diimine and dithiolate) lying on the same plane. On the other hand, the four donor atoms (2N and 2S) are not co-planar in complex **8** [35,36]. The chelating coordination of the pq ligand introduces a strain in the molecule, which may results to the tetrahedral distortion of the coordination plane (the PtN<sub>2</sub>/PtS<sub>2</sub> dihedral angle is 8.9°). Although this contribution could be attributed to the asymmetry of the pq ligand, in all the solved crystal structures of free pq and its Cu(I) and (II), Zn(II), Hg(II), Mo(0) and W(0) complexes, pq is planar [63–68]. Thus, the dithiolate ligand must play an important role moving the S atom close to the C (H) of pq ligand (Fig. 1) resulting to tetrahedral distortion. This distortion has a significant role in the biological properties of complex **8** since it affects on its electronic and stacking properties [35,36]. This steric distortion reduces the

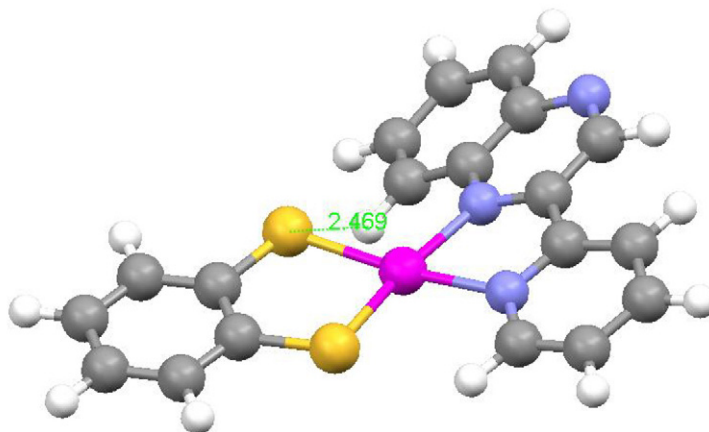


Fig. 1. Molecular structure of **8**. The atom distance among the atoms S and the H is indicated by the dash line.

**Table 2**

DFT calculated one electron energies and composition of selected highest occupied and lowest unoccupied orbitals of MOs of M(diimine)(dithiolate) expressed in terms of composing fragments for complexes **1–8**.

Complex	MO	E (eV)			
<b>1</b>	LUMO+1(a <sub>2</sub> )	−3.23	99.4	0.2	0.4
	LUMO(b <sub>1</sub> )	−3.41	94.8	2.8	2.4
	HOMO(b <sub>1</sub> )	−5.47	3.8	86.3	9.8
	HOMO-1(a <sub>2</sub> )	−6.60	1.4	75.5	23.1
<b>2</b>	LUMO+1(a <sub>2</sub> )	−2.73	99.3 (99.2)	0.2 (0.3)	0.5 (0.5)
	LUMO(b <sub>1</sub> )	−2.89	92.8 (92.3)	4.3 (4.6)	2.9 (3.1)
	HOMO(b <sub>1</sub> )	−4.66	5.4 (6.4)	85.6 (84.8)	9.0 (8.8)
	HOMO-1(a <sub>2</sub> )	−5.11	0.9 (1.0)	88.8 (88.4)	10.3 (10.6)
<b>3</b>	LUMO+1(a <sub>2</sub> )	−2.08	99.0 (99.1)	0.3 (0.2)	0.8 (0.7)
	LUMO(b <sub>1</sub> )	−2.93	92.4 (92.1)	4.6 (4.8)	3.0 (3.1)
	HOMO(b <sub>1</sub> )	−4.69	5.8 (6.0)	85.4 (85.4)	8.8 (8.7)
	HOMO-1(a <sub>2</sub> )	−5.14	0.8 (0.8)	89.1 (89.0)	10.1 (10.1)
<b>4</b>	LUMO+1(a <sub>2</sub> )	−2.08	98.9	0.1	1.0
	LUMO(b <sub>1</sub> )	−2.93	91.4	5.3	3.3
	HOMO(b <sub>1</sub> )	−4.67	6.5	84.2	9.3
	HOMO-1(a <sub>2</sub> )	−5.14	0.7	89.1	10.3
<b>5</b>	LUMO+1(a <sub>2</sub> )	−2.04	98.1 (98.2)	0.5 (0.3)	1.4 (1.5)
	LUMO(b <sub>1</sub> )	−2.92	87.4 (87.1)	7.2 (7.4)	5.4 (5.6)
	HOMO(b <sub>1</sub> )	−4.63	10.0 (10.1)	79.9 (79.8)	10.0 (10.1)
	HOMO-1(a <sub>2</sub> )	−5.13	1.7 (1.8)	83.7 (83.4)	14.6 (14.8)
<b>6</b>	LUMO+1(a <sub>2</sub> )	−1.92	98.1	0.5	1.4
	LUMO(b <sub>1</sub> )	−2.81	84.6	9.7	5.6
	HOMO(b <sub>1</sub> )	−4.50	12.7	78.0	9.3
	HOMO-1(a <sub>2</sub> )	−5.68	3.0	67.4	29.6
<b>7</b>	LUMO+1(a <sub>2</sub> )	−2.59	98.3	0.4	1.2
	LUMO(b <sub>1</sub> )	−3.49	90.4	5.0	4.5
	HOMO(b <sub>1</sub> )	−5.51	7.5	81.1	11.4
	HOMO-1(a <sub>2</sub> )	−6.53	2.8	67.0	30.2
<b>8</b>	LUMO+1(a <sub>2</sub> )	−2.19	98.5	0.5	1.0
	LUMO(b <sub>1</sub> )	−3.37	83.1	9.9	7.1
	HOMO(b <sub>1</sub> )	−4.98	13.4	75.8	10.8
	HOMO-1(a <sub>2</sub> )	−5.39	1.6	84.0	14.4

In parenthesis the calculated values with polarization function for Pd and Pt are given.

chemical nuclease activity of pq ligand of **8** in comparison to the bis(dihydroquinoxaline)copper(II) analogues [69] without affecting the photonuclease activity of complex **8** [70]. The latter is of importance in the chemistry of photodynamic therapy of cancer.

A similar effect on planar structure is observed in the case of Pt(3,3'-dcbpy)(mnt) complex which having an almost tetrahedral structure, gives better efficiency on dye-sensitized solar cells than the similar square-planar Pt(4,4'-dcbpy)(mnt) [33]. Both cases are well reproduced by DFT calculations [36,71].

Inspecting the data in Table 1, one can easily conclude that M–N bond lengths are longer than those observed in bis-diimine compounds, while M–S distances have been contracted, as compared to those of the related bis-dithiolenes [62]; this is a consequence of significant *trans*-influence effect.

The identity of the metal atom seems to have an influence both on the M–S and M–N bond lengths as we can observed by inspecting the data in Table 1 for complexes **3–5**. Thus, the M–N bond lengths increase in the order Ni–N < Pt–N < Pd–N; Ni has a significantly smaller bonding radii as compared to Pd and Pt. According to the contribution of each fragment and the relative energies of bonding orbitals (Table 2), we can conclude that the better overlap between the metal atom and the dithiolate ligand in Pd complexes reduces the electron density of the M–N bonds. On the other hand, as both Pd<sup>2+</sup> and Pt<sup>2+</sup> have almost the same radius (86 and 85 pm, respectively), they can successively overlap with both conjugated ligands, thus providing the series Ni–S > Pd–S ~ Pt–S on passing from Ni to Pt.

## 2.2. Electronic transitions and excited states of M(diimine)(dithiolate) complexes: effect of metal, ligands and solvent

### 2.2.1. Ground and singlet states

All M(diimine)(dithiolate) complexes exhibit broad and partially structured long-wavelength absorption bands. These bands show negative solvatochromism, indicating their charge-transfer character. Earlier experimental studies have assigned the lowest allowed electronic transition of this class of compounds as LL/CT [43,92], as MMLL/CT [37] while recently the general term 'charge transfer-to-diimine' has been employed [13]. The assignment MMLL/CT was confirmed by our TD-DFT study [38,60] in the case of the neutral M(diimine)(dithiolate), where M = Ni, Pd and Pt. This has been further proven for similar mixed diimine–dithiolato or thiocyanato compounds as Pt[X,X'-(COOEt)<sub>2</sub>-bpy](mnt) where X = 3, 4 or 5 [71], Pt(4-COOCH<sub>3</sub>-py)<sub>2</sub>(mnt) [72], Pt(SCN)<sub>2</sub>(bpy) [73] and a series of azobenzene-conjugated dithiolato–bipyridine Pt(II) complexes [74].

As we have already mentioned, our calculations were performed with Gaussian 98 and 03 software. The Stuttgart–Dresden (SDD) basis set was used with a relativistic effective core potential for Pd and Pt and all light atoms were described by the all-electron 6-31G\* basis set. Electronic absorption spectra of complexes **1–8** are generally well reproduced by TD-DFT calculations, but only if the solvent is included; thus the hybrid B3LYP function was used together with CPCM correction for all solvents under study.



In order to assign the absorption bands, and in particular to determine the metal, diimine and dithiolate ligand contributions to the highest occupied MOs (HOMO) as well as the solvent effect, DFT calculations were performed on all the aforementioned complexes (**1–8**). The orbital energies along with the contributions from the two ligands, namely diimine and dithiolene, and the metal are given in Table 2. In all complexes the two highest occupied orbitals are denoted mainly dithiolate/metal in character, while no pure  $d_{\text{metal}}$  orbitals have been observed [38,71,72]. This is in accordance with the non innocent nature of the dithiolate ligand that causes large d–d splittings. As a consequence, the HOMO, a  $b_1$  orbital, is composed mainly of sulfur  $3p_z$  orbitals that form antibonding interactions with metal  $d_{xz}$  orbitals and carbon  $2p_z$  orbitals on the chelating ring. On the other hand, LUMO is calculated to be almost exclusively located on diimine whereas a limited contribution of metal and dithiolate ligand still exists. More precisely, apart from the interactions between carbon atoms of the carbohydrate core, antibonding interactions of the  $2p_z$  nitrogen orbitals with the  $d_{xz}$  metal orbital are also present. The aforementioned motive is consistent with  $\pi^*$ -back-bonding theory, indicating that electron back-donation to phen or bpy is reduced by the presence of dithiolate as compared with other diimine complexes [40]. Although, inspecting Table 2, the prevailing character of HOMO and LUMO is dithiolate and diimine, respectively, the admixture of metal in both orbitals and their percentage difference must be acknowledged since this reflects on differences in the properties (electrochemical and photophysical ones) of these complexes.

The role of the nature of the dithiolate in the electronic structure of the M(diimine)(dithiolate) complexes, is examined in **5–7** complexes (Table 2). The criterion of  $\pi^*$ -accepting ability of the substituents to the dithiolate chelating ring is satisfied. More precisely,  $-\text{CN}$  is a good  $\pi^*$ -accepting group as compared to  $-\text{H}$ , whereas bdt is a widely used aromatic ligand. Earlier experimental work [13,23,43] has indicated that electron accepting groups stabilize HOMO; this has fully supported by our DFT calculations for complexes under study and the HOMO is stabilized in the order  $\text{mnt}^{2-} > \text{bdt}^{2-} > \text{edt}^{2-}$ . The same series is kept for the stabilization of LUMO. Moreover the participation of both metal and dithiolate orbitals in the latter is enhanced in consequence with  $\pi^*$ -back-bonding theory. Both trends enlarge the HOMO–LUMO gap (1.71 eV for **5** to 1.69 eV for **6** and 2.03 eV for **7**), in accordance with the observed UV–vis spectra.

Complexes **3** to **5** reveal the role of the metal. The data in Table 2 show that the contribution of the metal is increased in both HOMO (10.0% for Pt compared to 9.3% for Ni and 8.8% for Pd) and LUMO (5.4% for Pt compared to 3.3% for Ni and 3.0% for Pd) going from **5** to **4** and **3**. This trend is attributed to the better metal–ligand overlap induced by the 5d-orbitals of Pt compared to 4d-orbitals of Pd and 3d-orbitals of Ni. HOMO destabilizes along the same series, causing the reduction of the HOMO–LUMO energy gap; a result that fits well with experimental results [13,60] and reinforces at the same time the mixed metal–ligand-to–ligand notation for the observed charge-transfer band. The involvement of the metal in both orbitals (HOMO and LUMO) has already demonstrated by electrochemical measurements [45]. Taking in account the fact that all the three complexes **3**, **4** and **5** have the same ligands, namely bpy and bdt, the differences in cathodic ( $-1.85\text{V}$ ,  $-1.83\text{V}$ ,  $-1.78\text{V}$ , for **3**, **4** and **5**, respectively) and anodic waves ( $+0.17$ ,  $+0.08$ ,  $+0.03$ , for **3**, **4** and **5**, respectively) indicate a prevailing ligand and metal-centered character especially in the oxidation process which is attributed to HOMO. On the other hand, the reduction process suggests a LUMO with a certain ligand character (namely bpy) whereas the metal contribution is minimized in the opposite series of the  $E_{\text{red}}$ .

The solvent effect modeled by CPCM procedure, is mainly focused on the HOMO–LUMO gap and on the composition of

**Table 3**

DFT calculated one electron energies and composition of selected highest occupied and lowest unoccupied orbitals of MOs of Pd(phen)(bdt) expressed in terms of composing fragments, using B3LYP function together with CPCM.

Solvent	MO	$E$ (eV)	Metal	Diimine	Dithiol
Vacuum	LUMO + 1( $a_2$ )	−2.73	0.5	99.3	0.2
	LUMO( $b_1$ )	−2.89	2.9	92.8	4.3
	HOMO( $b_1$ )	−4.66	9.0	5.4	85.6
	HOMO−1( $a_2$ )	−5.11	10.3	0.9	88.8
$\text{C}_6\text{H}_6$	LUMO + 1( $a_2$ )	−2.65	0.5	99.3	0.2
	LUMO( $b_1$ )	−2.84	2.5	94.8	2.7
	HOMO( $b_1$ )	−4.93	9.9	3.7	86.3
	HOMO−1( $a_2$ )	−5.38	11.2	0.9	87.9
$\text{CHCl}_3$	LUMO + 1( $a_2$ )	−2.60	0.5	99.4	0.2
	LUMO( $b_1$ )	−2.80	2.3	95.5	2.2
	HOMO( $b_1$ )	−5.09	10.5	3.2	86.4
	HOMO−1( $a_2$ )	−5.55	11.8	0.9	87.3
$\text{CH}_3\text{CN}$	LUMO + 1( $a_2$ )	−2.55	0.5	99.4	0.2
	LUMO( $b_1$ )	−2.78	2.2	96.0	1.8
	HOMO( $b_1$ )	−5.22	10.8	2.9	86.3
	HOMO + 1( $a_2$ )	−5.68	12.2	0.9	86.9

HOMOs [60]. Actually, on going from non-polar to polar solvents, the HOMO–LUMO gap increases in accordance with experimental results and the negative solvatochromism (Table 3). Besides, the metal contribution in HOMO (for e.g. **2**) increases from 9.0% (in vacuum or benzene) to 10.8% (in  $\text{CH}_3\text{CN}$ ) (Table 3). This increase is pronounced in HOMO−1 to HOMO−4 orbitals [38,60] which at the same time exhibit larger dithiolate and less diimine character. On the contrary, the diimine character is greater in LUMO.

As we have already stated, the UV–vis spectra of all these complexes are supported by TD-DFT calculations [38,60]. Their spectra consist of three bands: one intense, solvatochromic band in the visible followed by a weaker solvent-independent in the near-UV and a third one in the UV-region. The highest energy transition was identified as diimine intraligand transitions whereas both the lower energy transitions were calculated to originate in MMLL/CT transitions from the dithiolate/metal moiety to the diimine ligand. In particular the lowest broad absorption band can be assigned to  $a^1A_1 \rightarrow b^1A_1$  transition, which is described mainly as a HOMO  $\rightarrow$  LUMO, whereas the higher lying band assigned to  $a^1A_1 \rightarrow e^1A_1$  (e.g. HOMO−4  $\rightarrow$  LUMO for **1** or HOMO−4  $\rightarrow$  LUMO + 1 for **5**). The solvent independence of the latter could attribute to the localization of the involved HOMOs orbitals on sulfur atoms and on the other to the high contribution of the metal  $d$  orbitals (42.8% and 68.4% for **1** and **5**, respectively) which diminishes  $\Delta\mu_{\text{ge}}$  (where  $\Delta\mu_{\text{ge}}$  is the difference in ground and excited state dipole moments) and hence the  $\Delta E_{\text{solv}}$  of the involved states [38].

Moreover, the higher oscillator strengths are observed for the platinum complexes comparing with the palladium and nickel ones, in accordance with the molar extinction coefficient [38,60]. This observation strongly supports metal orbital involvement in the charge-transfer to diimine excited state since it could indicate the higher participation of the metal to charge-transfer procedure due to the greater metal  $d$ -orbital content. The higher oscillator strengths, combined with larger  $\lambda_{\text{max}}$  values for the Pt complexes, lead to materials with higher hyperpolarizability and make Pt(diimine)(dithiolate) complexes feasible candidates for materials with enhanced NLO properties [50,60], whereas if an effective charge separation is required, the order  $\text{Pd} > \text{Ni} > \text{Pt}$  must be kept. Eisenberg and co-workers [13] showed this experimentally using EFISH (electric field induced second harmonic) experiments on the compounds  $\text{M}(\text{dpphen})(\text{tbcda})$  and  $\text{M}(\text{dpphen})(\text{mncda})$ , with  $\text{M} = \text{Pd}, \text{Pt}$ . Moreover, experimental and theoretical results (DFT calculations) for a similar class of compounds such as the  $[\text{M}(\text{Me}(2)\text{pipdt})(\text{dmit})]$  complex based on

**Table 4**

TD-DFT calculated energies and compositions of the lowest lying singlet and triplet energy states together with oscillator strengths of Pt(diimine)(dithiolate) complexes [38].

C	State		Composition <sup>a</sup>	$\Delta E^b$	$f^c$	Character
5	b <sup>1</sup> A <sub>1</sub>	Singlet	9b <sub>1</sub> (HOMO) → 10b <sub>1</sub> (LUMO), 78%	1.53	0.15	bdt/Pt → bpy (MMLL/CT)
	b <sup>3</sup> A <sub>1</sub>	Triplet	9b <sub>1</sub> (HOMO) → 11b <sub>1</sub> (LUMO + 1), 100%	2.02		bdt/Pt → bpy (MMLL/CT)
6	b <sup>1</sup> A <sub>1</sub>	Singlet	8b <sub>1</sub> (HOMO) → 9b <sub>1</sub> (LUMO), 71%	1.48	0.13	edt/bpy/Pt → bpy(MMLL/CT)
	a <sup>3</sup> B <sub>2</sub>	Triplet	6a <sub>2</sub> (HOMO–1) → 9b <sub>1</sub> (LUMO), 95%	1.94		edt/Pt → bpy(MMLL/CT)
			8b <sub>1</sub> (HOMO) → 7a <sub>2</sub> (LUMO + 2), 3%			
7	B <sup>1</sup> A <sub>1</sub>	Singlet	9b <sub>1</sub> (HOMO) → 10b <sub>1</sub> (LUMO), 83%	1.68	0.13	mnt/Pt → bpy (MMLL/CT)
		Triplet	9b <sub>1</sub> (HOMO) → 9a <sub>2</sub> (LUMO + 4), 67%	2.22		mnt/Pt → mnt (MLCT)
			9b <sub>1</sub> (HOMO) → 8a <sub>2</sub> (LUMO + 2), 28%			mnt/Pt → bpy(MMLL/CT)
			8b <sub>1</sub> (HOMO–3) → 9a <sub>2</sub> (LUMO + 4), 7%			mnt/Pt → mnt (MLCT)

<sup>a</sup> Compositions of electronic transitions are expressed in terms of contributing excitations between ground-state Kohn–Sham molecular orbitals.<sup>b</sup> Transition energy from the  $a^1A_1$  ground state in eV.<sup>c</sup> Oscillator strength.

the push Me(2)pidpt (1,4-dimethyl-piperazine-3,2-dithione) and pull dmit (1,3-dithiolo-2-thione-4,5-dithiolato) where M = Pd, Ni, points out that these complexes are potential second-order non-linear chromophores, whose properties are tunable with the metal [75,76].

### 2.2.2. Triplet states and emission spectra

TD-DFT can be used to calculate not only the singlet but also the triplet excited states for a closed-shell molecule, provided that the transition energies are smaller than the vertical ionization potential [48]. One of the very first studies for this purpose was our contribution for the triplet states of M(diimine)(dithiolate) [60]; after that a lot of papers demonstrated the applicability of TD-DFT calculation in transition metal complexes ([48,77] and references therein).

According to experimental results, none of the mixed diimine–dithiolate Pd or Ni complexes luminescent [60,78], whereas some Pt(diimine)(dithiolate) complexes exhibit long-lived emission spectra. The former could be attributed to strong interactions with solvent in the case of Pd and Ni complexes and/or non-totally symmetric distortions (due to the smaller contribution of Ni/Pd nd orbitals to both HOMOs and LUMOs), which could play an important role in non-radiative decay.

The lowest lying singlet and triplet energy state of complexes **5–7**, are given in Table 4. The character of the triplet excited states is related to the nature of the dithiolate ligand. Thus, while the emitting state of **5** is the triplet  $b^3A_1$  giving the  $^3[\text{bdt}/\text{M} \rightarrow \text{bpy}]$  and is in consistent with the MMLL/CT character of the transition, the emitting triplet state of Pt(bpy)(mnt), **7** is  $c^1A_1 \rightarrow b^3B_2$  at 2.22 eV (Fig. 2). In other words, the emission band of **7** comes mainly from a state of  $^3[\text{mnt}/\text{Pt} \rightarrow \text{mnt}]$  with only 28% of  $^3[\text{mnt}/\text{Pt} \rightarrow \text{bpy}]$  character referred as a MLCT/MMLL/CT transition (Table 4).

## 3. Calculated indices at DFT level for M(diimine)(dithiolate) complexes

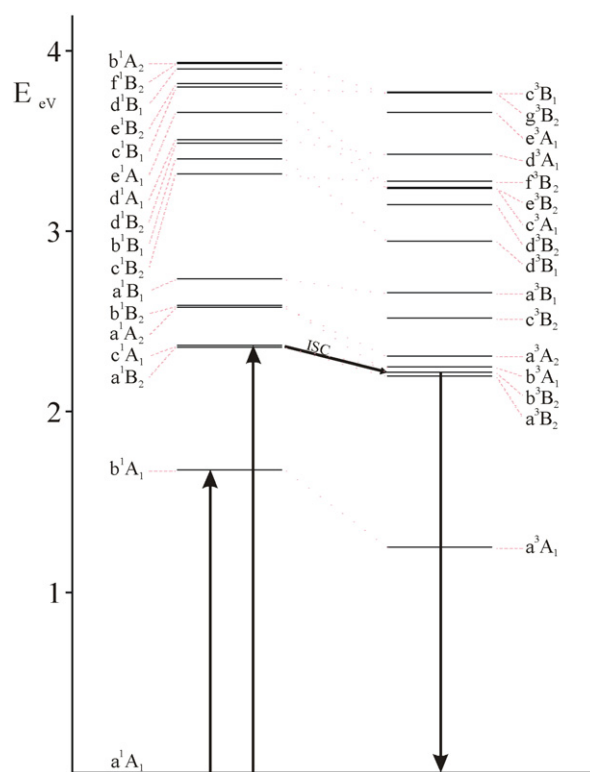
### 3.1. The NICS index: measuring the extent of the delocalization in the molecular plane

NICS values have been defined by von Rague Schleyer et al. [79] and are based on the absolute magnetic shieldings computed at ring center at ab initio, DFT, and semiempirical (MNDO) levels; the signs are reversed to conform to the NMR chemical shift convention (negative upfield and positive downfield). Significantly negative NICS values in interior positions of ring or cages indicate aromaticity or diatropic ring currents, whereas positive values denote antiaromaticity or paratropic ring currents [79]. Moreover,  $\sigma$ -contribution can be separated from  $\pi$ - one by using NICS(1) instead of NICS(0) [80]. NICS(1) refer to the location 1 Å above the center of ring plane; thus, local contributions of  $\sigma$ -bonds are reduced in favor of the  $\pi$ -effects. NICS is widely used to characterize aromaticity and

antiaromaticity of organic rings [81] but also, it is well-accepted as one of the most efficient tools for the understanding and interpretation of ring currents [80] of organics compounds, boranes and fullerenes [82], inorganic [83] and organometallic [84,85] complexes.

The importance of metalloaromaticity for further understanding of the degree of communication between the metal center and the chelating rings has been stressed repeatedly in many fields from biological electron transfer processes to materials design. Metalloaromaticity stabilizes coordinated chelate ligands, affects  $\pi$ -electron distribution and allows electrophilic substitution reaction to take place in the ligand. Moreover, both spectroscopic and magnetic properties of these complexes are effected by the degree of the aromaticity [86–88].

NICS index was used as a meter of the changes of the diatropic current in different M(diimine)(dithiolate) [49] and the extent of the delocalization in this class of compounds. A typical example of calculated NICS(0) and NICS(1) in a M(diimine)(dithiolate) complex



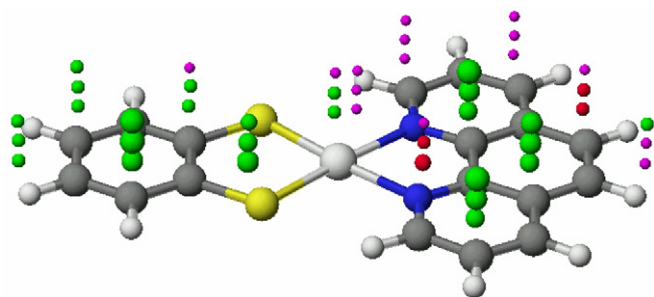


Fig. 3. Graphic representation of NICS values for the selected grid for Pd(phen)(bdt). Green spheres: diatropicity. Red spheres: paratropicity. Purple spheres: atropicity.

is demonstrated in Fig. 3. According to these results, the aromaticity of five membered dithiolate conjugated ring is marginal, whereas the relative diimine chelated ring can be generally characterized as non aromatic. Moreover, electron withdrawing groups as substituents to the dithiolate coordinated ring tend to enhance its diatropicity and have the opposite effect on the diimine chelated ring. Thus, in the series 5–7 the NICS(1) values of the five membered dithiolate ring decrease in the order  $7 > 5 > 6$  indicating the enhanced ring diatropicity in the presence of substituents with relatively high electron withdrawing ability. This is a consequence of the stabilization of HOMO caused by the electron withdrawing groups on dithiolate ring and the HOMO–LUMO gap, as has already referenced in the previous section. NICS also reveal the role of the metal indicating its significance in complexes' aromaticity and provide us with a proof of the involvement of the metal in the HOMO orbitals of these complexes. Thus, the diatropic ring current of the dithiolate (bdt) five member chelated ring decreases in the order  $4 > 5 > 3$  while the corresponding one for the (bpy) diimine conjugated ring, decreases in the order  $5 > 3 \sim 4$  in accordance with the energy of the MMLL/CT of these complexes. The former order was also derived for a series of bis(dithiolene) complexes [89] and is indicative of the contribution of the metal to the delocalized  $\pi$ -electron system. The above differences can only be due to the metal since both chelating ligands are the same for all the three complexes. The fact that the NICS(1) values are negative for the chelating ring of bdt indicates not only a diatropic current but mainly proves the involvement of the d orbitals of the metal to the delocalization  $\pi$ -electron system.

Moreover, the evolution of the NICS during complexation is consistent with the evolution of the diatropicity of the rings and implies the direction of the charge-transfer transition [49]. On the other hand, the reverse direction of  $^1\text{H}$  NMR and NICS(1) values upon complexation is indicative of the paratropic effect of the metal atom. The asymmetrical charge distribution in the valence orbitals of the metal is responsible to a large extent for the strong diamagnetic shift of the nucleus bound to it.

More recently, NICS have also be used to demonstrate the extent of the 'non-innocent' character of the dithiolene ligand in the case of the complexes  $[\text{CpCo}(\text{S}_2\text{C}_2(\text{H})\text{Ph})]$ ,  $[\text{CpCo}(\text{S}_2\text{C}_2(\text{H})\text{Ph})(\text{PMe}_3)]$ ,  $[\text{Au}(\text{S}_2\text{C}_2(\text{H})\text{Ph})_2](-)$  and  $[\text{Au}(\text{S}_2\text{C}_2(\text{H})\text{Ph})_2]$  [90]. Besides, the widespread applicability of NICS indices is also demonstrated in search of the baird and ray-dutt twist mechanisms of acemisation of Sc(III), Ti(III), Co(III), Zn(II), Ga(III), and Ge-IV complexes with a ligand analogue of acetylacetonate [91].

### 3.2. Fukui functions: searching the reactive centers in a molecule

In recent years, much attention has been paid to the insights that density functional theory can give into chemical reactivity and although electron density plays a fundamental role since it explains the reagent attacks on the basis of electrostatic interactions, it is

not enough. The main reason is that the influence induced by the approaching reagent is not estimated. Therefore, global reactivity parameters such as electronegativity ( $\chi$ ), hardness ( $\eta$ ) and electrophilicity index ( $\omega$ ) accompanied by local indices like the local softness and the Fukui function ( $f(\mathbf{r})$ ) have been introduced in the chemical literature [92–94] and eventually obtained legitimacy within DFT [94]. The latter has been proposed by Parr and Yang [95–98] and definitely represents one of the most effective tools of conceptual DFT for the investigation of the molecular reaction sites. The Fukui functions are frequently employed for the interpretation of factors and trends that influence the reacting behaviour of organic molecules, but more rarely used in the case of transition metal complexes [99–101].

In a recent study [50], we have demonstrated the usefulness of condensed Fukui functions in locating the preferred sites (atoms) for nucleophilic and electrophilic attack in the mixed (diimine)(dithiolate) complexes and predicting/explaining the products (even the minor ones) obtained during a reaction. The studied cases are referred especially to the addition of oxygen and other electrophiles as unsaturated compounds of Ag(I) or Au(II) compounds on mixed diimine–dithiolene complexes.

In general, we found a good agreement between the results obtained for the condensed Fukui indices of  $\text{M}(\text{diimine})(\text{dithiolate})$

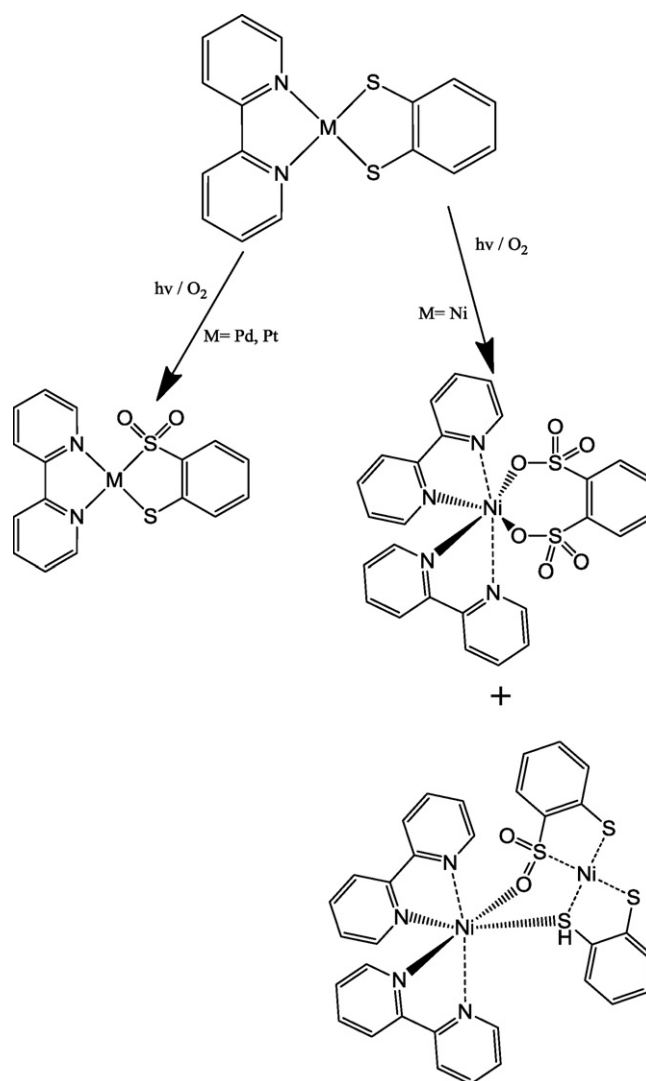
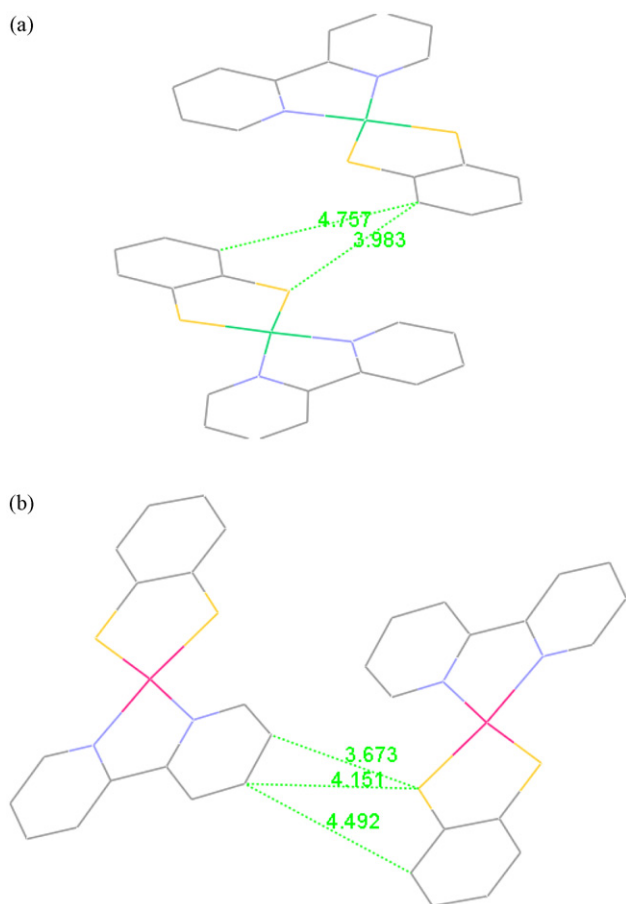


Fig. 4. Oxidation products of  $\text{M}(\text{bpy})(\text{bdt})$ ,  $\text{M} = \text{Ni}, \text{Pd}, \text{Pt}$  are different due to their Fukui functions.



**Fig. 5.** Packing of two molecules in molecular crystals of (a) Ni(bpy)(bdt) and (b) Pd(bpy)(bdt).

complexes and the experimental results upon electrophilic attack, i.e. oxidative process. The electrophilic attack occurs at a unique atomic site – namely, sulphur atom – in the M(diimine)(dithiolate) when the central metal is Pt or Pd. On the contrary, when mixed diimine–dithiolate of nickel is under consideration, the reactive sites except of sulphur atom, are the carbons of the dithiolene ring. Different reactive sites upon changing the central metal are reflected in the differences products obtained (Fig. 4). The HOMO is the orbital through which any oxidation process or electrophilic attack should take place. Thus, we suggest that metal is not just the right connector between two conductors but its role is essential for the reactivity of this class of compounds. Moreover, the nucleophilicity of sulphur atoms has been shown to increase in the series phen ~ bpy; mnt > edt > bdt and Pt > Ni > Pd for complexes 2–7.

Going further, our calculated Fukui functions for these complexes indicate that interactions of electrophile–nucleophile type are expected during crystal packing. This throws light on the different way the molecules can stack in a crystal lattice for complexes carrying the same ligands but different metal (2–5) in contrast to the  $\pi$  stacking theory. Fig. 5 shows the stacking of the Ni(bpy)bdt (a) and Pd(bpy)(bdt) (b) complexes [51]. Although these two complexes carrying the same ligands and as a consequence owning almost the same  $\pi$ -system, the way they are packed in crystal is different. Both complexes have been crystallized by the same system of solvents and no molecule of solvent has been co-crystallised. Actually, the Ni complex is crystallised in a head to head mode whereas Pd complex is packed in a head to tail mode. This variation certainly reflects on the different nucleophile–electrophile centers of the two complexes and the soft–soft interactions and underlines

the role of the metal in delocalisation system of the two conjugated five member ligands. This has further examined in a series of coordinated compounds of a sulfonated monoazo dye [102].

#### 4. Conclusions

DFT techniques give insight into the geometry and electronic structure of a series of mixed diimine–dithiolate complexes whereas TD-DFT calculates vertical transitions and reproduces absorption spectra very well especially when the polarized continuum model is taken in account. Moreover, TD-DFT can be used to calculate the triplet excited states of these complexes. Thus, calculations performed on a wide range of M(diimine)(dithiolate) complexes point to mixed characters of the low-lying transitions and excited states, which are described as MMLL/CT (mixed metal–ligand-to–ligand charge transfer). The metal and ligands contributions vary with the nature of metal, the substituents of the ligands, the structure of the complex and the medium. Polar solvents generally favour larger charge separation upon excitation.

The contribution of the metal in the chemical and photophysical properties of this class of compounds is also demonstrated by two indices derived by DFT techniques: NICS and Fukui functions. NICS is a measure of the diatropic current in a molecule or in other words of the delocalization over this class of molecules—providing us with a theoretical tool of the non-innocent character of the dithiolate ring and the role of the metal. Moreover, the evolution of the NICS during complexation is consistent with the evolution of the diatropicity of the rings and implies the direction of the charge-transfer transition. On the other side, Fukui functions identify the reactive centres of the molecule upon electrophilic or nucleophilic reagents. The differences on Fukui indices in accordance with the experimental data reveal the importance of metal and its contribution to the electronic structure of the M(diimine)(dithiolate) complexes. Thus, compounds with the same ligands but different metal (of the same group) result to different products under the same circumstances. Besides, Fukui indices provide us with an alternative to  $\pi$ -stacking explanation of the same class of compounds.

All the theoretical results are in accordance with the experimental ones, indicating the superiority of the DFT and TD-DFT techniques in examining the properties (electronic and photophysics) of a series of donor–acceptor transition metal complexes and selecting between mixed–diimine–dithiolate complexes for their use as photosensitizers, NLO materials, light energy conversion materials and biological reagents.

#### Acknowledgements

Special thanks are attributed to Dr. C. Makedonas, Dr. I. Veroni, Dr. C. Dagas and Dr. F. Lahoz since this contribution would not have been possible without their invaluable work. Financial support from EU COST D35 Action is gratefully acknowledged.

#### References

- [1] V.P. Mueller-Westerhoff, D.I. Yoon, *Tetrahedron* 47 (1991) 440.
- [2] R. Battaglia, R. Henning, B. Dinh-Ngoc, W. Schlamann, H. Kisch, *J. Mol. Catal.* 21 (1983) 239.
- [3] E. Vrachnou, C. Mitsopoulou, D. Katakis, J. Konstantatos, in: D.O. Hall, G. Grassi (Eds.), *Photoconversion Processes for Energy and Chemicals: Energy from Biomass*, vol. 5, Elsevier Applied Science, 1989, p. 1098.
- [4] C. Mitsopoulou, J. Konstantatos, D. Katakis, E. Vrachnou, *J. Mol. Catal.* 67 (1991) 137.
- [5] D. Katakis, C. Mitsopoulou, J. Konstantatos, E. Vrachnou, P. Falaras, *J. Photochem. Photobiol. A: Chem.* 68 (1992) 375.
- [6] D. Katakis, C. Mitsopoulou, E. Vrachnou, *J. Photochem. Photobiol. A: Chem.* 81 (1994) 103.
- [7] E. Lyris, D. Argyropoulos, C. Mitsopoulou, D. Katakis, E. Vrachnou, *J. Photochem. Photobiol. A: Chem.* 108 (1997) 51.



- [8] R. Humphry-Baker, C.A. Mitsopoulou, D. Katakis, E. Vrachnou, J. Photochem. Photobiol. A: Chem. 114 (1998) 137, 3.
- [9] J. Samios, D. Katakis, D. Dellis, E. Lyras, C.A. Mitsopoulou, J. Chem. Soc., Faraday Trans. 94 (1998) 3169.
- [10] W. Paw, S.D. Cummings, M.A. Mansour, W.B. Connick, D.K. Geiger, R. Eisenberg, Coord. Chem. Rev. 171 (1998) 125.
- [11] M. Hissler, J.E. McGarrah, W.B. Connick, D.K. Geiger, S.D. Cummings, R. Eisenberg, Coord. Chem. Rev. 208 (2000) 115.
- [12] C.-T. Chen, S.-Y. Liao, K.-J. Lin, L.-L. Lai, Adv. Mater. 3 (1998) 334.
- [13] D.K. Cummings, L.-T. Cheng, R. Eisenberg, Chem. Mater. 9 (1997) 440.
- [14] R.S. Pilato, E.I. Stiefel, in: J. Reedijk (Ed.), Bioinorganic Catalysis, Marcel Dekker, New York, 1998.
- [15] G.N. Schrauzer, Acc. Chem. Res. 2 (1969) 72.
- [16] J.A. McCleverty, Prog. Inorg. Chem. 10 (1968) 49.
- [17] D. Argyropoulos, C.A. Mitsopoulou, D. Katakis, Inorg. Chem. 35 (1996) 5549.
- [18] D. Argyropoulos, E. Lyras, C.A. Mitsopoulou, D. Katakis, J. Chem. Soc. Dalton Trans. (1997) 615.
- [19] R.P. Burns, C.A. McAuliffe, Adv. Inorg. Chem. Radiochem. 22 (1979) 303.
- [20] P. Falaras, C. Mitsopoulou, D. Argyropoulos, E. Lyras, E. Vrachnou, D. Katakis, N. Psaroudakis, Inorg. Chem. 34 (1995) 4536.
- [21] C.A. Mitsopoulou, E. Lyras, S. Veltsos, D. Katakis, Inorg. React. Mech. 3 (2001) 99.
- [22] E.I. Stiefel, in: K.D. Karlin (Ed.), Dithiolene Chemistry: Synthesis, Properties and Applications, Prog. Inorg. Chem., vol. 52, 2004.
- [23] T.R. Miller, I.G. Dance, J. Am. Chem. Soc. 95 (1973) 6970.
- [24] S. Huertas, M. Hissler, J.E. McGarrah, R.J. Lachicotte, R. Eisenberg, Inorg. Chem. 40 (2001) 1183.
- [25] W.B. Connick, D. Geiger, R. Eisenberg, Inorg. Chem. 38 (1999) 3264.
- [26] W. Paw, R.J. Lachicotte, R. Eisenberg, Inorg. Chem. 37 (1998) 4139.
- [27] J.A. Zuleta, M.S. Burberry, R. Eisenberg, R. Coord. Chem. Rev. 97 (1990) 47.
- [28] J.A. Zuleta, C.A. Chesta, R. Eisenberg, J. Am. Chem. Soc. 111 (1989) 8916.
- [29] G. Matsubayashi, M. Nakano, H. Tamura, Coord. Chem. Rev. 226 (2002) 143.
- [30] V.E. Kaasjager, E. Bouwman, S. Gorter, J. Reedijk, C.A. Grapperhaus, J.H. Reibenspies, J.J. Smee, M.Y. Darensbourg, A. Derecskei-Kovacs, L.M. Thomson, Inorg. Chem. 41 (2002) 1837.
- [31] J. Si, Q. Yang, Y. Wang, P. Ye, S. Wang, J. Qin, D. Lin, Opt. Commun. 132 (1996) 311.
- [32] A. Islam, H. Sugihara, K. Hara, L.P. Singh, R. Katoh, M. Yanakida, Y. Takahashi, S. Murata, H. Arakawa, Inorg. Chem. 40 (2001) 5371.
- [33] E.A.M. Geary, J. Yellowlees, L.A. Jack, I.D.H. Oswald, S. Parsons, N. Hirata, J.R. Durrant, N. Robertson Inorg. Chem. 44 (2005) 242.
- [34] C.A. Mitsopoulou, G. Lappa, E. Stathatos, P. Lianos, unpublished results.
- [35] C.A. Mitsopoulou, C. Dagas, C. Makedonas, Inorg. Chim. Acta 361 (2008) 1973.
- [36] C.A. Mitsopoulou, C.E. Dagas, C. Makedonas, J. Inorg. Biochem. 102 (2008) 77.
- [37] S.D. Cummings, R. Eisenberg, Inorg. Chem. 34 (1995) 2007.
- [38] C. Makedonas, C.-A. Mitsopoulou, F.J. Lahoz, A.I. Balana, Inorg. Chem. 42 (2003) 8853.
- [39] C.E. Keefer, R.D. Bereman, S.T. Purrington, B.W. Knight, P.D. Boyle, Inorg. Chem. 38 (1999) 2294.
- [40] A. Vlček Jr., Coord. Chem. Rev. 230 (2002) 225.
- [41] C. Makedonas, C.A. Mitsopoulou, Eur. J. Inorg. Chem. (2007) 110.
- [42] C. Makedonas, I. Veroni, C.A. Mitsopoulou, Eur. J. Inorg. Chem. (2007) 120.
- [43] K.H. Puthraya, T.S. Srivastava, Tetrahedron 4 (1985) 1579.
- [44] Y. Zhang, K.D. Ley, K.S. Schanze, Inorg. Chem. 35 (1996) 7102.
- [45] T.M. Cocker, R.E. Bachman, Inorg. Chem. 40 (2001) 1550.
- [46] W.B. Connick, H.B. Gray, J. Am. Chem. Soc. 119 (1997) 11620.
- [47] B.S. Lim, D.V. Fomitchev, R.H. Holm, Inorg. Chem. 40 (2001) 4257.
- [48] A. Vlček Jr., S. Zláliš, Coord. Chem. Rev. 251 (2007) 258.
- [49] C. Makedonas, C.A. Mitsopoulou, Eur. J. Inorg. Chem. (2006) 2460.
- [50] C. Makedonas, C.A. Mitsopoulou, Eur. J. Inorg. Chem. (2006) 590.
- [51] Cambridge Structural Database, Chem. Des. Autom. News 8 (1993) 31.
- [52] M. Buhl, C. Reimann, D.A. Pantazis, T. Bredow, F. Neese, J. Chem. Theory Comput. 4 (2008) 1449.
- [53] A.D. McLean, G.S. Chandler, J. Chem. Phys. 72 (1980) 5639.
- [54] R. Krishnan, J.S. Binkley, R. Seeyer, J.A. Pople, J. Chem. Phys. 72 (1980) 650.
- [55] D. Andrae, U. Haeussermann, M. Dolg, H. Stoll, H. Preuss, Theor. Chim. Acta 77 (1990) 123.
- [56] K.A. Peterson, D. Figgen, M. Dolg, H. Stoll, J. Chem. Phys. 126 (2007) 124101.
- [57] C. Makedonas, C.A. Mitsopoulou, Unpublished results.
- [58] C.J. Adams, N. Fey, M. Parfitt, S.J.A. Pope, J.A. Weinstein, Dalton Trans. (2007) 4446.
- [59] L. Petit, P. Maldivi, C. Adamo, J. Chem. Theor. Comput. 1 (2005) 953.
- [60] C. Makedonas, C.A. Mitsopoulou, Inorg. Chim. Acta 360 (2007) 3997.
- [61] W. Koch, M.C. Holthausen, A Chemist's Guide to Density Functional Theory, 2nd ed., Wiley-VCH Verlag GmbH, Weinheim, 2001.
- [62] J.M. Bevilacqua, R. Eisenberg, Inorg. Chem. 33 (1994) 2913.
- [63] I. Veroni, C. Makedonas, A. Rontoyianni, C.A. Mitsopoulou, J. Organomet. Chem. 691 (2006) 267.
- [64] C. Makedonas, I. Veroni, C.A. Mitsopoulou, J. Eur. Inorg. Chem. (2007) 120.
- [65] E. Veroni, A. Rontoyianni, C.A. Mitsopoulou, Dalton Trans. 2 (2003) 255.
- [66] I. Veroni, C.A. Mitsopoulou, F.J. Lahoz, J. Organomet. Chem. 691 (2006) 5955.
- [67] I. Veroni, C.A. Mitsopoulou, F.J. Lahoz, J. Organomet. Chem. 693 (2008) 2451.
- [68] S.P. Perlepes, A. Garoufis, J. Sletten, E.G. Bakalbassis, G. Plakatouras, E. Katsarou, N. Hadjiliadis, Inorg. Chim. Acta 261 (1997) 93.
- [69] D.S. Sigman, Acc. Chem. Res. 19 (1986) 180.
- [70] A.R. Chakravarty, J. Chem. Sci. 118 (2006) 443.
- [71] E.A.M. Geary, K.L. McCall, A. Turner, P.R. Murray, E.J.L. McInnes, L.A. Jack, L.J. Yellowlees, N. Robertson, Dalton Trans. (2008) 3701.
- [72] L.P. Moorcraft, A. Morandeira, J.R. Durrant, J.R. Jennings, L.M. Peter, S. Parsons, A. Turner, L.J. Yellowlees, N. Robertson, Dalton Trans. (2008) 6940.
- [73] X.-Y. Hu, X.-J. Liu, J.-K. Feng, Chin. J. Chem. 25 (2007) 1370.
- [74] R. Sakamoto, S. Kume, M. Sugimoto, H. Nishihara, Chem. Eur. J. 15 (2009) 1429.
- [75] L. Pilia, F. Artizzu, C. Faulmann, M.L. Mercuri, A. Serpe, P. Deplano, Inorg. Chem. Commun. 12 (2009) 490.
- [76] S. Curreli, P. Deplano, C. Faulmann, A. Ienco, C. Mealli, M.L. Mercuri, L. Pilia, G. Pintus, A. Serpe, E.F. Trogu, Inorg. Chem. 43 (2004) 5069.
- [77] S.R. Stoyanov, J.M. Villegas, D.P. Rillema, Inorg. Chem. Commun. 7 (2004) 838.
- [78] W.L. Ffleman, W.B. Connick, Comments Inorg. Chem. 23 (2002) 205.
- [79] P.V.R. Schleyer, C. Maerker, A. Drausfeld, H. Jiao, N.J.R.V.E. Hommes, J. Am. Chem. Soc. 118 (1996) 6317.
- [80] P.V.R. Schleyer, M. Manoharan, Z.-X. Wang, B. Kiran, H. Jiao, R. Puchta, N.J.R.V.E. Hommes, Org. Lett. 316 (2001) 2465.
- [81] A.A. Fokin, H. Jiao, P.V.R. Schleyer, J. Am. Chem. Soc. 120 (1998) 9364.
- [82] A. Hirsch, Z. Chen, H. Jiao, Angew. Chem. Int. Ed. 39 (2000) 3915.
- [83] P.V.R. Schleyer, B. Kiran, D.V. Simon, T.S. Sorensen, J. Am. Chem. Soc. 122 (2000) 510.
- [84] P.V.R. Schleyer, H. Jiao, N.J.R.V.E. Hommes, V.G. Malkin, O.L. Malkina, J. Am. Chem. Soc. 119 (1997) 12669.
- [85] G. Liu, Q. Fang, C.C. Wang, J. Mol. Struct. (THEOCHEM) 679 (2004) 115.
- [86] H. Masui, Coord. Chem. Rev. 219 (2001) 957.
- [87] H. Masui, A.B.P. Lever, E.S. Dodsworth, Inorg. Chem. 32 (1993) 258.
- [88] A.B.P. Lever, H. Masui, R.A. Metcalfe, D.J. Stufkens, E.S. Dodsworth, P.R. Auburn, Coord. Chem. Rev. 125 (1993) 317.
- [89] C. Lauterbach, J. Fabian, Eur. J. Inorg. Chem. (1999) 1995.
- [90] G. Periyasamy, N.A. Burton, I.H. Hillier, M.A. Vincent, H. Disley, J. McMaster, D.C. Garner, Faraday Discuss. 135 (2007) 469.
- [91] H.S. Rzepa, M.E. Cass, Inorg. Chem. 46 (2007) 8024.
- [92] A. Vogler, H. Kunkely, J. Am. Chem. Soc. 103 (1981) 1559.
- [93] P.W. Ayers, M. Levy, Theor. Chem. Acc. 103 (2000) 353.
- [94] P. Geerlings, F. De Proft, W. Langenaeker, Chem. Rev. 103 (2003) 1793.
- [95] P.W. Ayers, J.S.M. Anderson, L.J. Bartolotti, Int. J. Quantum Chem. 101 (2005) 520.
- [96] R.G. Parr, W. Yang, Density Functional Theory of Atoms and Molecules, Oxford University Press, Oxford, 1989.
- [97] R.G. Parr, W. Yang, J. Am. Chem. Soc. 106 (1984) 4049.
- [98] W. Yang, R.G. Parr, R. Pucci, J. Chem. Phys. 81 (1984) 2862.
- [99] K. Fukui, Science 218 (1982) 747.
- [100] A. Ríos-Escudero, I. Costamagna, G.I. Cárdenas-Jirón, J. Phys. Chem. A 108 (2004) 7253.
- [101] C. Makedonas, C.A. Mitsopoulou, Eur. J. Inorg. Chem. (2007) 4176.
- [102] J. Lue, S.-Y. Gao, J.-X. Lin, L.-X. Shi, R. Cao, S.R. Batten, Dalton Trans. (2009) 1944.